Environ. Sci. Technol. **2000**, *34,* 2513−2517

Low-Dose Responses to 2,3,7,8-Tetrachlorodibenzo-*p*-dioxin in Single Living Human Cells Measured by Synchrotron Infrared Spectromicroscopy

HOI-YING N. HOLMAN,*,† REGINE GOTH-GOLDSTEIN,‡ MICHAEL C. MARTIN,§ MARION L. RUSSELL,‡ AND WAYNE R. MCKINNEY§

Center for Environmental Biotechnology, Environmental Energy Technologies Division, and Advanced Light Source Division, Lawrence Berkeley National Laboratory, 1 Cyclotron Road, Berkeley, California 94720

Synchrotron radiation (SR)-based Fourier transform infrared (FTIR) spectromicroscopy measurements are presented of HepG2 cells exposed to an environmental contaminant that is a known ligand for the aryl hydrocarbon (Ah) receptor. Measurements were made on cells treated with an Ah receptor-binding model compound 2,3,7,8-tetrachlorodibenzo-*p*-dioxin (TCDD). Compared to untreated control cells, treated cells displayed unique spectral changes with TCDD concentrations of 0.01−10.0 nM. Key spectral changes involved P═O, C−O, and C−H stretching bands. The first changes are related to the environment of the phosphate backbone of nucleic acids. The C−H stretching bands data show a relative increase in the number of methyl to methylene groups. An excellent correlation was found between spectral changes and an increase in *CYP1A1* expression measured by the reverse transcriptase polymerase chain reaction (RT-PCR) technique demonstrating that the SR−FTIR method is observing cellular biochemical changes related to this gene expression pathway. Finally, the potential use of SR−FTIR spectromicroscopy is discussed as a diagnostic tool for monitoring cellular exposure and early molecular responses to environmental pollutants.

Introduction

Exposure to polychlorinated aromatic compounds can lead to various health effects including cancers, alteration of hormone levels, and reproductive defects in animals (*1*−*6*) and humans (*7*−*14*). Among this family of pollutants, 2,3,7,8-tetrachlorodibenzo-*p*-dioxin (TCDD) is one of the most potent and most studied "man-made" toxins, causing harmful effects at exposure levels of hundreds or thousands of times lower than most chemicals of environmental concern (*15*). TCDD acts by binding to the aryl hydrocarbon (Ah) receptor (*16, 17*). Binding triggers induction of various genes involved in xenobiotic metabolism including the cytochrome P4501A1 (*CYP1A1*) gene (*16*−*20*). In the risk management of polychlorinated aromatic compounds, frequently the induction of cellular responses (such as the induced expression of *CYP1A1*) are measured using slot blot, Northern blot, Western blot (*21*), or the reverse transcription polymerase chain reaction (RT-PCR) technique that employs gene-specific primers (*6, 22, 23*). This approach involves techniques that require fairly large numbers of cells, is destructive to the cells, and requires lengthy sample preparations including DNA or RNA purification and amplification and/or other chemical and enzymatic treatments before their final analysis.

An alternative to the above analytical, chemical, and biochemical techniques is microcopy methods where processes in the intact cells or tissues are investigated. These include electron microscopies (*24*−*26*), soft X-ray microscopies (*27, 28*), optical fluorescence microscopy (*29*−*31*), and its recent extension using multiphoton excitation (*32*−*40*). However, many of these methods are harmful to living cells, and most require treatments with exogenous dyes, fluorescent labels, or stains. Synchrotron radiation (SR)-based Fourier transform infrared (FTIR) spectromicroscopy does not share the requirement for labels, while the method rapidly and nondestructively probes individual living cells and provides, in addition, chemical information from the IR spectrum (*41*).

Conventional non-SR-based FTIR spectromicroscopy has been widely used as a diagnostic tool for characterizing the composition and structure of cellular components within intact tissues (*42*−*45*) and for measuring tumor tissue responses to therapy (*46*). However, the spatial resolution of traditional FTIR spectromicroscopy is limited to ∼75 μm with sufficient signal-to-noise (*47, 48*). SR−FTIR spectromicroscopy, on the contrary, provides several hundred times higher brightness at a diffraction-limited spatial resolution of 10 μm or better and is therefore a sensitive analytical technique capable of providing molecular information on biological specimens (*47*−*51*). In a recent example, Jamin et al. (*41*) used SR−FTIR to map the distribution of functional groups of biomolecules such as proteins, lipids, and nucleic acids in individual live cells with a spatial resolution of a few microns. In this study, we use SR−FTIR spectromicroscopy to measure directly intracellular responses to TCDD.

Experimental Details

The SR−FTIR spectromicroscopy experiments began with exposing HepG2 cells (derived from a human hepatocellular carcinoma) to various concentrations of TCDD. A fraction of the exposed cells were investigated by acquiring SR−FTIR spectra from individual live cells. The remaining cells were analyzed for *CYP1A1* gene expression, using the RT-PCR technique. Observed changes in the SR−FTIR spectral measurements were compared with those from RT-PCR results.

Cells and Cell Treatment. HepG2 cells were selected for use in this study as their ability to metabolize polyaromatic compounds is well-characterized (*52*). HepG2 cells were obtained from the American Tissue Culture Collection (Rockville, MD). They were maintained in Dulbecco's minimum essential medium supplemented with 10% fetal calf serum, nonessential amino acids, 1 mM L-glutamine, 10 mM *N*-(2-hydroxyethyl)piperazine-*N*′-(2-ethanesulfonic acid) (HEPES), and antibiotics. Cells were subcultured every 7 days. For TCDD experiments, subconfluent cultures were exposed for 20 h to 10^{-11}, 10^{-10}, and 10^{-9} M TCDD initially dissolved in pure dimethyl sulfoxide (DMSO) (Sigma, USA, 99.9% pure).

* Corresponding author e-mail: hyholman@lbl.gov; telephone: (510)486-5943; fax: (510)486-7152.
† Center for Environmental Biotechnology.
‡ Environmental Energy Technologies Division.
§ Advanced Light Source Division.

10.1021/es991430w CCC: $19.00
Published on Web 05/11/2000

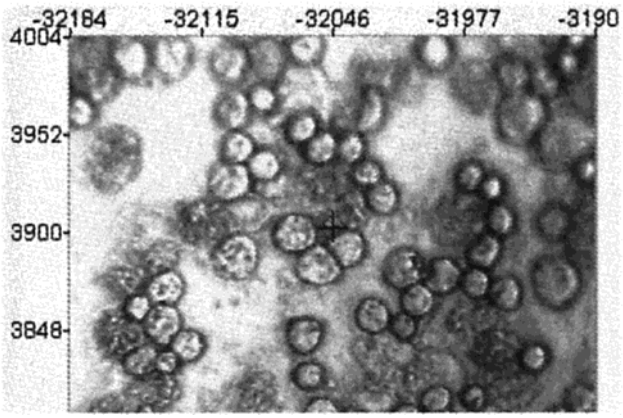

FIGURE 1. Video-captured photomicrograph acquired through the infrared microscope of trypsinized HepG2 cells placed on a gold surface and ready for SR−FTIR analysis. The axes labels are the position of the microscope *x*−*y* stage (in μm).

For the control experiment, subconfluent cultures remained in the incubator for 20 h without exposure to TCDD.

At the end of the 20-h treatments, cells were either harvested for SR−FTIR analysis or lysed using TRI Reagent (Sigma, USA) for RT-PCR studies. Harvesting cells for SR−FTIR analysis was done by trypsinizing and washing twice in ice-cold phosphate-buffered saline (PBS). These cell suspensions were kept at 4 °C and measured with SR−FTIR within 24 h. Cells from suspension were pipetted onto a chilled reflecting gold surface for double-pass transmission SR−FTIR analysis. This preparation provided round cells with many separated individuals as shown in Figure 1. Cells with a diameter of ~20 μm were visually selected for spectral analysis to narrow the distribution with respect to cell cycle (*53*).

SR−FTIR Spectromicroscopy. The infrared spectromicroscopy facility on Beamline 1.4.3 (*49*) at the Advanced Light Source (ALS), Lawrence Berkeley National Laboratory (LBNL), was used to monitor intracellular changes in response to TCDD exposure. The infrared microprobe uses a synchrotron source that has much higher brightness than a conventional thermal IR source. The synchrotron light is incident into a Nicolet Magna 760 FTIR bench and then is passed through a Nic-Plan IR microscope. The spot size of the unmasked synchrotron beam focused through the infrared microscope is ≤10 μm, approximately diffraction-limited, and significantly smaller than the ~100-μm spot size attainable using a conventional thermal IR source. This leads to an improved signal-to-noise level and finer spatial resolution than is possible for FTIR spectromicroscopy with conventional sources (*47*−*49*). Since mid-infrared light is low in energy and, as such, is nondestructive to biological materials, SR−FTIR spectromicroscopy is extremely useful in detecting subtle intracellular changes in live cells as they are exposed to environmental stimuli.

All SR−FTIR spectra were recorded in the 4000−650-cm^{-1} infrared region as this mid-IR region contains unique molecular absorption fingerprints (e.g., 54). Every IR measurement consisted of 128 co-added spectra at a spectral resolution of 4 cm^{-1}. All spectra were obtained in the double-pass transmission geometry and ratioed to the spectrum of a bare gold-coated slide, and absorbance values were computed. The center of each cell was found to within an accuracy of ~±2 μm by acquiring a line-map across each individual cell and then using the most absorbing, and therefore the thickest, part of the cell for analysis. Any residual water vapor features in the resultant spectrum were removed by subtracting an appropriately scaled reference spectrum of water vapor. To account for cell to cell thickness variations,

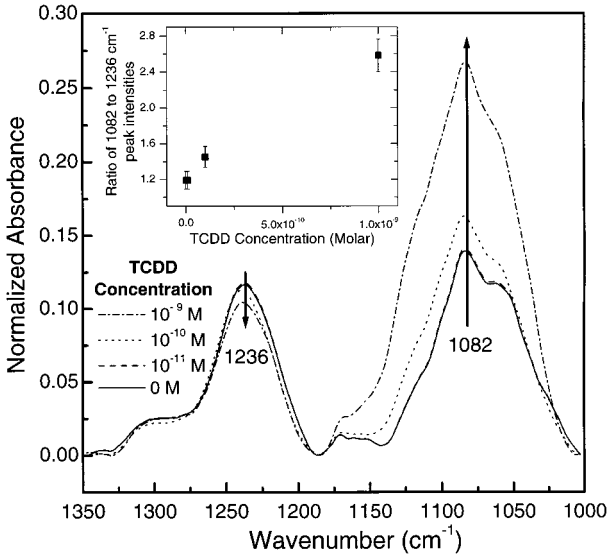

FIGURE 2. Infrared spectra in the phosphate band region for cells treated with 0, 10^{-11}, 10^{-10}, and 10^{-9} M TCDD. Spectra have been normalized to the protein amide II peak intensity to account for cell to cell thickness variations. Inset shows the ratio of the 1082−1236 cm^{-1} peak intensities as a function of TCDD concentration.

the final spectrum from each cell was normalized with the protein amide II peak (1548 cm^{-1}). The amide II band has been used as an internal standard for total cell mass and shown to follow Beer's law in studies of biomolecules (*55*). Spectra from up to five cells from each dosage treatment were obtained to ensure reproducibility. These spectra were then averaged, and any scatter in the spectral results is presented as error bars in the data analysis. Typically the spectral features of interest reproduced to within a few percent.

Semiquantitative RT-PCR. Total RNA was isolated from cell cultures from each TCDD dosage using TRI Reagent (Sigma, USA). Total RNA was reverse transcribed using oligo dT, MMLV reverse transcriptase. CYP1A1 expression was measured by determining the CYP1A1 transcript level relative to a constantly expressed internal control gene, the β-actin gene (*56*). Primers designed to span an intron were used to generate PCR products. PCR conditions and cycle numbers were optimized for each target sequence to ensure that the reaction was in the linear phase of product accumulation. After being amplified, the products were separated by electrophoresis on a polyacrylamide gel. The gel was stained with SYBR gold fluorescent stain (Molecular Probes, Inc., USA) and scanned on a Molecular Dynamics STORM 860 laser scanner. The fluorescent signal for each band was quantified using ImageQuant software (Molecular Dynamics, USA).

Results

The overall absorbance spectral features of biological materials are well-known (*41*, *42*, *45*, *57*), and cellular SR−FTIR spectra of this study follow the established pattern. However, by comparing spectra from cells treated with various amounts of TCDD to untreated cells, significant spectral differences were found in the magnitude and, in some cases, the location of peaks at various wavelengths. The present analysis concentrates on changes observed in the phosphate band region (1350−1000 cm^{-1}) and the C−H band region (3050−2800 cm^{-1}).

Phosphate Bands. Figure 2 shows the IR spectra of unexposed HepG2 cells (solid line) and of cells exposed to different concentrations of TCDD in the phosphate band region. For untreated cells the two phosphate absorption

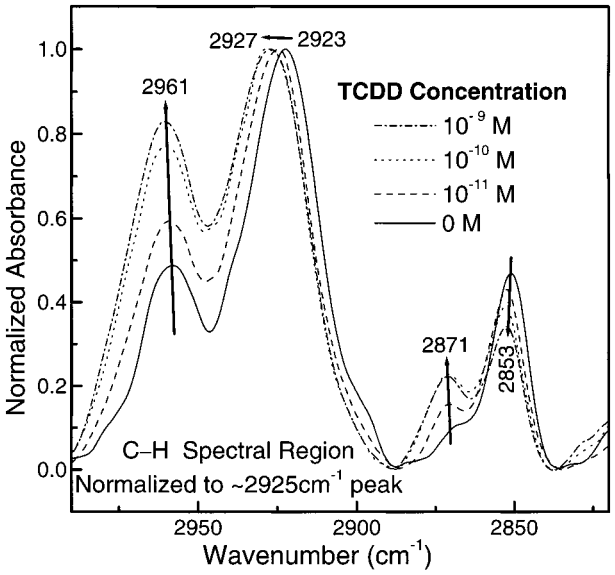

FIGURE 3. Infrared spectra in the C−H stretching vibration region for cells treated with 0, 10^{-11}, 10^{-10}, and 10^{-9} M TCDD. Spectra have been normalized to the ~2925 cm^{-1} peak height.

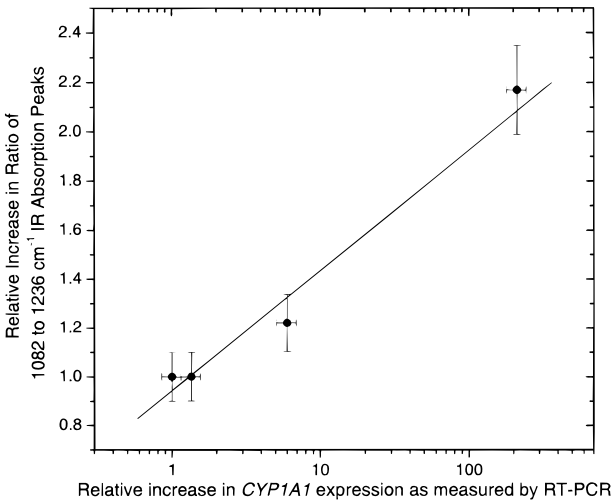

FIGURE 4. Comparison of results from SR−FTIR analysis of the phosphate band absorptions and the increase in *CYP1A1* expression as measured by RT-PCR.

bands (*44, 45*) at 1236 cm^{-1} (asymmetric phosphate stretching mode ν_{as} PO_2^-) and at 1082 cm^{-1} (symmetric phosphate stretching mode ν_s PO_2^-) were approximately equal in strength. For TCDD-treated HepG2 cells, the ν_{as} PO_2^- band decreased somewhat in intensity while the ν_s PO_2^- band increased by more than a factor of 2 for the highest TCDD doses studied. There were no detectable frequency shifts of either phosphate stretching mode for TCDD treatments studied. As shown in the inset to Figure 2, the intensity ratio of the ν_s PO_2^- to ν_{as} PO_2^- peaks increased with TCDD concentration.

The 1145−1190 cm^{-1} region showed a small peak that is associated with a C−O vibration (*45*). This band seemed to increase in intensity with increasing TCDD concentration. This C−O mode was observed to shift in studies of cancerous colorectal (*44*) and breast tissues (*58*).

C−H Bands. Spectral absorptions due to hydrocarbon vibrations in lipids, proteins, nucleic acids, sugars, and phosphates among others were found within the 3050−2800-cm^{-1} region. Figure 3 displays the SR−FTIR spectra of unexposed HepG2 cells (solid line) and of cells exposed to different concentrations of TCDD in the C−H stretch region normalized to the peak maximum near 2925 cm^{-1}. The band near 2853 cm^{-1} is due to the symmetric CH_2 stretching mode of the methylene chains in membrane lipids; the peak at ~2925 cm^{-1} is due to the asymmetric CH_2 stretch; 2961 cm^{-1} absorption is due to asymmetric stretching of the CH_3 methyl groups of both lipids and proteins; and the 2871-cm^{-1} mode is from the symmetric CH_3 stretching mode (*44, 57, 59*). For TCDD-treated HepG2 cells, the 2853 peak decreased in intensity while the 2961- and 2871-cm^{-1} peaks increased. This indicates that the ratio of the number of methyl groups to that of methylene groups increases as the TCDD concentration increases. All C−H bands shown in Figure 3 were observed to stiffen with increased TCDD exposure.

Comparison of SR−FTIR and RT-PCR. RT-PCR was carried out on extracts from the cell cultures of each TCDD exposure concentration as described above. Measured values of *CYP1A1* gene expression were normalized to measured β-actin levels, and finally the relative increase in *CYP1A1* as a function of TCDD was obtained. The above systematic spectral changes obtained by SR−FTIR spectromicroscopy were compared with results from the RT-PCR technique. This comparison was done to determine if the SR−FTIR spectral changes can be associated with intracellular changes due to the induction of the *CYP1A1* gene. The relative increase in the ratio of the symmetric to asymmetric phosphate infrared bands with increasing TCDD concentration was compared to the relative increase in *CYP1A1* induction in Figure 4. Error bars for the IR data arose from the fact that we measured at 5 or less cells for each treatment concentration. The solid line in Figure 4 is a weighted linear regression fit to the data. The excellent agreement (with $r^2 = 0.96$) for measurements from the two methods indicates that the rapid SR−FTIR spectromicroscopy technique can measure biochemical changes due to the *CYP1A1* expression processes.

Discussion

Several previous infrared studies on normal and diseased human tissues have observed spectral changes in the phosphate bands region. A study of sickle red blood cell membranes (*60*) showed a splitting and shift in the symmetric P═O stretch band from 1080 cm^{-1} in normal cells to 1060 and 1090 cm^{-1} in sickle cells and a downshift of the asymmetric phosphate band by 30 cm^{-1}. The authors of that study hypothesized that this may be due to increased oxidative stresses in the membranes of sickle cells causing changes in the packing of the membrane lipids. A colorectal cancer tissue study (*44, 61*) and a lung cancer cell study (*62*) found that the asymmetric peak softened while the symmetric peak stiffened in the malignant samples as compared to normal samples. In addition, they observed a significant increase in the ratio of the 1082−1236 cm^{-1} peaks similar to our observations in the inset of Figure 2.

Generally the asymmetric PO_2^- vibration is at 1240 cm^{-1} when it is non-hydrogen-bonded and 1220 cm^{-1} when highly hydrogen-bonded (*61*). Our data show that this band as well as the symmetric phosphate band do not shift at any TCDD dose studied. Therefore, we can conclude that the hydrogen-bonding environment of the phosphate backbone of nucleic acids in the HepG2 cells is weak and remains unchanged throughout the study. This contrasts with the previous cancerous tissue studies where this hydrogen-bonding is observed to increase (*61, 62*).

As noted in the discussion of Figure 3, the relative change in intensities of the C−H stretching vibrations indicates that the number of methyl groups is increased as compared to methylene groups upon exposure to TCDD. The opposite has been found in colorectal cancer tissue analysis (*44, 61*). Other authors have proposed that TCDD removes the protection from methylation from certain sites when it binds

to the Ah receptor (*63*) or that increased methylation may downregulate the expression of the *CYP1A1* gene (*64*). Since methylation is so intimately involved with gene inactivation (*65*) and a significant increase in the number of methyl groups produced after exposure to TCDD was observed, potentially indicating increased methylation, this could explain the tremendous toxicity of TCDD in humans and other animals.

The data presented demonstrate the ability of the SR−FTIR technique to measure clear spectral changes in cells that have been exposed to low concentrations of TCDD, which triggers the Ah receptor-mediated pathway. However, this study was limited in that only a limited number of cells per data point of a single cell type were measured. Even with this small sampling we are confident that using SR−FTIR to observe subtle changes in individual cells will provide new understanding. Future studies will investigate changes in many different types of cells as well as cellular biochemical processes resulting from a variety of agents. While the infrared spectra of whole cells are quite complex and it is extremely difficult to assign the changes observed to specific molecular events, the use of cell lines that are defective in a single process or pathway may allow specific mechanisms to be identified in the spectra and studied comprehensively. Once a better understanding of how to interpret IR spectral changes is accomplished, infrared spectromicroscopy may be developed into a rapid and inexpensive diagnostic tool for medical screening applications. The single cell nature of this technique may allow identification of a small number of viable cells in a population that are different from the others, potentially opening new areas of environmental health and biomedical research.

Acknowledgments

This work was performed with support by the Directors, Office of Energy Research, Office of National Petroleum Technology Program, Offices of Health and Environmental Sciences, Biological and Environmental Research Program and Basic Energy Sciences, Materials Science Division, of the United States Department of Energy under Contract DE-AC03-76SF00098. Treatment of cells with TCDD was done in the laboratory of Prof. Leonard Bjeldanes of the University of California at Berkeley with the help of Dr. Jacque Riby. We thank Drs. Eleanor Blakely and Terry Hazen for numerous helpful discussions.

Literature Cited

(1) Lee, B. M.; Strickland, P. T. *Immunol. Lett.* **1993**, *36*, 117−123.
(2) Wang, J.-S.; Busby, W. F. *Carcinogenesis* (*Oxford*) **1993**, *14*, 1871−1874.
(3) Chaloupka, K.; Steinberg, M.; Santostefano, M.; Rodriguez, L. V.; Goldstein, L.; Safe, S. *Chem.-Biol. Interact.* **1995**, *96*, 207−221.
(4) Borm, P. J. A.; Knaapen, A. M.; Schins, R. P. F.; Godschalk, R. W. L.; Schooten, F.-J. V. *Environ. Health Perspect.* **1997**, *105*, 1089−1093.
(5) Nesnow, S.; Ross, J. A.; Stoner, G. D.; Mass, M. J. *Toxicology* **1995**, *105*, 403−413.
(6) Walker, N. J.; Portier, C. J.; Lax, S. F.; Crofts, F. G.; Li, Y.; Lucier, G. W.; Sutter, T. R. *Toxicol. Appl. Pharmacol.* **1999**, *154*, 279−286.
(7) Perera, F. P.; Tang, D. L.; O'Neill, J. P.; Bigbee, W. L.; Albertini, R. J.; Santella, R.; Ottman, R.; Tsai, W. Y.; Dickey, C. *Carcinogenesis* (*Oxford*) **1993**, *14*, 969−973.
(8) Omland, O.; Sherson, D.; Hansen, A. M.; Sigsgaard, T.; Autrup, H.; Overgaard, E. *Occup. Environ. Med.* **1994**, *51*, 513−518.
(9) Kang, D. H.; Rothman, N.; Poirier, M. C.; Greenberg, A.; Hsu, C. H.; Schwartz, B. S.; Baser, M. E.; Groopman, J. D.; Weston, A.; Strickland, P. T. *Carcinogenesis* (*Oxford*) **1995**, *16*, 1079−1085.
(10) Farmer, P. B.; Sepai, O.; Lawrence, R.; Autrup, H.; Nielsen, P. S.; Vestergard, A. B.; Waters, R.; Leuratti, C.; Jones, N. J.; Stone, J.; Baan, R. A.; Van Delft, J. H. M.; Steenwinkel, M. J. S. T.; Kyrtopoulos, S. A.; Souliotis, V. L.; Theodorakopoulos, N.; Bacalis, N. C.; Natarajan, A. T.; Tates, A. D.; Haugen, A.; Andreassen, A.; Ovrebo, S.; Shuker, D. E. G.; Amaning, K. S.; Schouft, A.; Ellul, A.; Garner, R. C.; Dingley, K. H.; Abbondandolo, A.; Merlo, F.; Cole, J.; Aldrich, K.; Beare, D.; Capulas, E.; Rowley, G.; Waugh, A. P. W.; Povey, A. C.; Haque, K.; Kirsch-Volders, M.; Van Hummelen, P.; Castelain, P. *Mutagenesis* **1996**, *11*, 363−381.
(11) Lewtas, J.; Walsh, D.; Williams, R.; Dodbias, L. *Mutat. Res.* **1997**, *378*, 51−63.
(12) Van Schooten, F. J.; Godschalk, R. W. L.; Breedijk, A.; Maas, L. M.; Kriek, E.; Sakai, H.; Wigbout, G.; Baas, P.; Van T Veer, L.; Van Zandwijk, N. *Mutat. Res.* **1997**, *378*, 65−75.
(13) Gustavsson, P.; Jakobsson, R.; Johansson, H.; Lewin, F.; Norell, S.; Rutkvist, L.-E. *Occup. Environ. Med.* **1998**, *55*, 393−400.
(14) Pan, G.; Hanaoka, T.; Yamano, Y.; Hara, K.; Ichiba, M.; Wang, Y.; Zhang, J.; Feng, Y.; Shujuan, Z.; Guan, D.; Gao, G.; Liu, N.; Takahashi, K. *Carcinogenesis* (*Oxford*) **1998**, *19*, 1963−1968.
(15) *Health Assessment for 2,3,7,8 tetrachlorodibenzo-p-dioxin (TCDD) and Related Compounds*; EPA600AP92001; U.S. Environmental Protection Agency: Washington, DC, 1997.
(16) Whitlock, J. P. *Annu. Rev. Pharmacol. Toxicol.* **1999**, *39*, 103−125.
(17) Safe, S. H. *Pharmacol. Ther.* **1995**, *67*, 247−281.
(18) Warshawsky, D.; Livingston, G. K.; Fonouni-Fard, M.; La Dow, K. *Environ. Mol. Mutagen.* **1995**, *26*, 109−118.
(19) Lang, D. S.; Becker, S.; Develin, R. B.; Koren, H. S. *Cell Biol. Toxicol.* **1998**, *14*, 23−38.
(20) Parrish, A. R.; Alejandro, N. F.; Bowes, R. C.; Ramos, K. S. *Toxicol. In Vitro* **1998**, *12*, 219−232.
(21) Runge-Morris, M.; Wilusz, J. *Toxicol. Appl. Pharmacol.* **1994**, *125*, 133−141.
(22) Vanden Heuvel, J. P.; Clark, G. C.; Thompson, C. L.; McCoy, Z.; Miller, C. R.; Lucier, G. W.; Bell, D. A. *Carcinogenesis* (*Oxford*) **1993**, *14*, 2003−2006.
(23) Abel, J.; Li, W.; Doehr, O.; Vogel, C.; Donat, S. *Naunyn-Schmiedeberg's Arch. Pharmacol.* **1996**, *353*, R127.
(24) Martone, M. E.; Deerinck, T. J.; Young, S. J.; Ellisman, M. H. *Acta Histochem. Cytochem.* **1999**, *32*, 35−43.
(25) Risco, C.; Carrascosa, J. L. *Histol. Histopathol.* **1999**, *14*, 905−926.
(26) Becker, W. M.; Reece, J. B.; Poenie, M. F. *The world of the cell*; Benjamin/Cummings: Menlo Park, CA, 1996.
(27) Jacobsen, C. *Trends Cell Biol.* **1999**, *9*, 44−48.
(28) Gilbert, E. S.; Khlebnikov, A.; Meyer-Ilse, W.; Keasling, J. D. *Water Sci. Technol.* **1999**, *39*, 269−272.
(29) Inglefield, J. R.; Schwartz-Bloom, R. D. *Methods* (*Orlando*) **1999**, *18*, 197−203.
(30) Darzynkiewicz, Z.; Bedner, E.; Li, X.; Gorczyca, W.; Melamed, M. R. *Exp. Cell Res.* **1999**, *249*, 1−12.
(31) Feng, D.; Nagy, J. A.; Pyne, K.; Hammel, I.; Dvorak, H. F.; Dvorak, A. M. *Microcirculation* (*New York*) **1999**, *6*, 23−44.
(32) Fricker, M. D.; Oparka, K. J. *J. Exp. Bot.* **1999**, *50*, 1089−1100.
(33) Centonze, V. E.; White, J. G. *Biophys. J.* **1998**, *75*, 2015−2024.
(34) Hasegawa, S. *Acta Histochem. Cytochem.* **1998**, *31*, 293−296.
(35) Kloppenburg, P.; Zipfel, W. R.; Webb, W. W.; Harris-Warrick, R. M. *Soc. Neurosci. Abstr.* **1998**, *24*, 1893.
(36) Mohler, W. A.; Williams-Masson, E.; White, J. G. *Biophys. J.* **1998**, *74*, A8.
(37) Nichols, J. A.; Webb, W. W. *Biophys. J.* **1998**, *74*, A189.
(38) Nichols, J. A.; Webb, W. W. *FASEB J.* **1998**, *12*, A947.
(39) Subramaniam, V.; Kirsch, A. K.; Schnetter, C.; Rivera-Pomar, R.; Arndt-Jovin, D.; Jovin, T. M. *Biophys. J.* **1998**, *74*, A227.
(40) Zipfel, W. R.; Kloppenburg, P.; Harris-Warrick, R. M.; Webb, W. W. *Biophys. J.* **1999**, *76*, A21.
(41) Jamin, N.; Dumas, P.; Moncuit, J.; Fridman, W.-H.; Teillaud, J.-L.; Carr, G. L.; Williams, G. P. *Proc. Natl. Acad. Sci. U.S.A.* **1998**, *95*, 4837−4840.
(42) Diem, M.; Boydston-White, S.; Chiriboga, L. *Appl. Spectrosc.* **1999**, *53*, 148A−161A.
(43) Griffiths, P. R.; De Haseth, J. A. *Fourier transform infrared spectrometry*; Wiley: New York, 1986.
(44) Rigas, B.; Morgello, S.; Goldman, I. S.; Wong, P. T. T. *Proc. Natl. Acad. Sci. U.S.A.* **1990**, *87*, 8140−8144.
(45) Parker, F. S. *Applications of infrared spectroscopy in biochemistry, biology, and medicine*; Plenum Press: New York, 1971.
(46) Stone, H. B.; Brown, J. M.; Phillips, T. L.; Sutherland, R. M. *Radiat. Res.* **1993**, *136*, 422−434.
(47) Choo, L.-P. I.; Wetzel, D. L.; Halliday, W. C.; Jackson, M.; Levine, S. M.; Mantsch, H. H. *Biophys. J.* **1996**, *71*, 1672−1679.
(48) Carr, G. L.; Reffner, J. A.; Williams, G. P. *Rev. Sci. Instrum.* **1995**, *66*, 1490−2.
(49) Martin, M. C.; McKinney, W. R. *Proceedings of the Materials Research Society*; Mini, S. M., Stock, S. R., Perry, D. L., Terminello, L. J., Eds.; 1998; Vol. 524, pp 11−15.

(50) Miller, L. M.; Carr, G. L.; Williams, G. P.; Chance, M. R. *Biophys. J.* **1997**, *72*, A214.
(51) Lappi, S.; Miller, L.; Chance, M.; Franzen, S. *Biophys. J.* **1999**, *76*, A354.
(52) Delescluse, C.; Ledirac, N.; De Sousa, G.; Pralavorio, M.; Botta-Fridlund, D.; Letreut, Y.; Rahmani, R. *Toxicol. In Vitro* **1997**, *11*, 443−450.
(53) Goth-Goldstein, R.; Burki, H. J. *Mutat. Res.* **1980**, *69*, 127−37.
(54) Liquier, J.; Taillandier, E. In *Infrared Spectroscopy of Biomolecules*; Mantsch, H. H., Chapman, D., Eds.; Wiley-Liss: New York, 1996; pp 131−158.
(55) Neumann, D.; Schultz, C. P.; Helm, D. In *Infrared Spectroscopy of Biomolecules*; Mantsch, H. H., Chapman, D., Eds.; Wiley-Liss: New York, 1996; pp 279−310.
(56) Goth-Goldstein, R.; Russell, M. *Proc. Am. Assoc. Cancer Res. Annu. Mtg.* **1999**, *40*, 570.
(57) Stuart, B.; Ando, D. J. *Biological applications of infrared spectroscopy*; Published on behalf of ACOL (University of Greenwich) by John Wiley: Chichester/New York, 1997.
(58) Malins, D. C.; Polissar, N. L.; Nishikida, K.; Holmes, E. H.; Gardner, H. S.; Gunselman, S. J. *Cancer* (*Philadelphia*) **1995**, *75*, 503−517.
(59) Wong, P. T. T.; Wong, R. K.; Caputo, T. A.; Godwin, T. A.; Rigas, B. *Proc. Natl. Acad. Sci. U.S.A.* **1991**, *88*, 10988−10992.
(60) Kucuk, O.; Lis, L. J.; Dey, T.; Mata, R.; Westerman, M. P.; Yachnin, S.; Szostek, R.; Tracy, D.; Kauffman, J. W.; et al. *Biochim. Biophys. Acta* **1992**, *1103*, 296−302.
(61) Rigas, B.; Wong, P. T. T. *Cancer Res.* **1992**, *52*, 84−88.
(62) Wang, H. P.; Wang, H. C.; Huang, Y. J. *Sci. Total Environ.* **1997**, *204*, 283−287.
(63) Carrier, F.; Chang, C.-Y.; Duh, J.-L.; Nebert, D. W.; Puga, A. *Biochem. Pharmacol.* **1994**, *48*, 1767−1778.
(64) Takahashi, Y.; Suzuki, C.; Kamataki, T. *Biochem. Biophys. Res. Commun.* **1998**, *247*, 383−386.
(65) Freifelder, D.; Malacinski, G. M. *Essentials of molecular biology*; Jones and Bartlett Publishers: Boston, 1993.

Received for review December 22, 1999. Revised manuscript received March 20, 2000. Accepted April 5, 2000.

ES991430W